Journal of Power Sources 185 (2008) 76–84

Contents lists available at ScienceDirect

Journal of Power Sources

journal homepage: www.elsevier.com/locate/jpowsour

Investigation of $Ba_{1-x}Sr_xCo_{0.8}Fe_{0.2}O_{3-\delta}$ as cathodes for low-temperature solid oxide fuel cells both in the absence and presence of CO_2

Aiyu Yan[a,b], Min Yang[a,b], Zhifang Hou[a], Yonglai Dong[a], Mojie Cheng[a,*]

[a] Dalian Institute of Chemical Physics, Chinese Academy of Sciences, Dalian 116023, China
[b] Graduate Schools of the Chinese Academy of Sciences, Beijing 100039, China

ARTICLE INFO

Article history:
Received 21 April 2008
Received in revised form 30 June 2008
Accepted 30 June 2008
Available online 15 July 2008

Keywords:
$Ba_{1-x}Sr_xCo_{0.8}Fe_{0.2}O_{3-\delta}$
Solid oxide fuel cell
Cathode
Carbon dioxide

ABSTRACT

$Ba_{1-x}Sr_xCo_{0.8}Fe_{0.2}O_{3-\delta}$ (BSCF)($0 \le x \le 1$) composite oxides were prepared and tested as cathodes for low-temperature solid oxide fuel cells (SOFCs) both in the absence and presence of CO_2. It is found that the BSCF cathodes in the whole range of strontium doping levels show promising performance at 500–600 °C in the absence of CO_2, among which the $SrCo_{0.8}Fe_{0.2}O_{3-\delta}$ (SCF) cathode gives the highest power density while $BaCo_{0.8}Fe_{0.2}O_{3-\delta}$ (BCF) cathode shows the lowest performance. The impedance analysis reveals that both the ohmic resistance and polarization resistance of the fuel cell increases when the strontium content decreases. It is believed that the microstructure and electrical conductivity simultaneously affect the process of oxygen reduction. The presence of CO_2 deteriorates the BSCF performance by adsorbing on the cathode surface and thus obstructing the oxygen surface exchange reaction. The CO_2 exerts a more intense influence on BSCF with higher barium content.

1. Introduction

Solid oxide fuel cell (SOFC) has emerged as one of the most important power generation technologies because of its high-energy-conversion efficiency and low pollution emission [1–4]. Low-temperature solid oxide fuel cell (LT-SOFC) is receiving growing interests recently due to its improved stability, reliability and reduced cost [5,6]. However, the challenge for LT-SOFCs is to develop high-performance cathode materials at low temperatures.

Mixed ionic and electronic conducting perovskite oxides, such as $La_{0.6}Sr_{0.4}CoO_{3-\delta}$, $La_{0.6}Sr_{0.4}Co_{0.8}Fe_{0.2}O_{3-\delta}$, $Sm_{0.5}Sr_{0.5}CoO_3$ and $Ba_{0.5}Sr_{0.5}Co_{0.8}Fe_{0.2}O_{3-\delta}$ (BSCF5582) [7–12], are of great interest as intermediate or low-temperature cathodes because they contain active oxygen reduction sites over the entire cathode surface. Currently, BSCF5582 represents one of the most promising cathode materials that has attracted considerable attention for its use in LT-SOFCs [12–18]. Haile group [12] reported that BSCF5582 displayed excellent performance at 400–600 °C in both dual and single chamber configurations. They further demonstrated its potential application as a cathode for a thermally self-sustained micro SOFC stack with high power density [13]. BSCF has good chemical compatibility with $Gd_xCe_{1-x}O_2$, $Sm_xCe_{1-x}O_2$ and $La_{1-x}Sr_xGa_{1-y}Mg_yO_3$ electrolytes which exhibit desirable ionic conductivity at low temperatures [12–17]. Baumann et al. [18] reported that the oxygen reduction reaction at geometrically well-defined BSCF5582 microelectrodes was limited by the oxygen surface exchange reaction and/or by the transfer of oxide ions across the electrode/electrolyte interface. Its resistance of electrochemical surface exchange was more than a factor of 50 lower than the corresponding value of $La_{0.6}Sr_{0.4}Co_{0.8}Fe_{0.2}O_{3-\delta}$ microelectrodes of the same geometry.

Although promising results were achieved, some drawbacks of BSCF were also reported. Recently, it was demonstrated that BSCF cathode or membrane could be deteriorated by even small amount of CO_2 [19–21] owing to its reaction with alkaline-earth elements resulting in the formation of Ba and Sr carbonates [20–21]. Therefore, it is necessary to take into account the stability of BSCF in atmosphere containing CO_2 since the presence of CO_2 is characteristic of the static air.

It is well known that the physical and chemical properties of the perovskite-type oxides could be modified by tuning the composition of A and B sites [22]. Recently, several groups described the influence of iron doping level in $Ba_{0.5}Sr_{0.5}Co_{1-y}Fe_yO_{3-\delta}$ on its phase structure, electrical conductivity and performance [23,24]. On the other hand, barium doping levels in A-site also affect the physical and chemical properties of BSCF by changing the oxygen vacancy concentration and valance of B-site cations in the bulk [25], resulting in the variety of the crystal structure, electrical conductivity and thermal expansion coefficients [25,27]. Since oxygen vacancies in the perovskite structure can contribute to the formation of the carbonate [28,29], altering the composition of A-site might also

* Corresponding author. Tel.: +86 411 84379049; fax: +86 411 84379049.
E-mail address: mjcheng@dicp.ac.cn (M. Cheng).

0378-7753/$ – see front matter © 2008 Elsevier B.V. All rights reserved.
doi:10.1016/j.jpowsour.2008.06.088

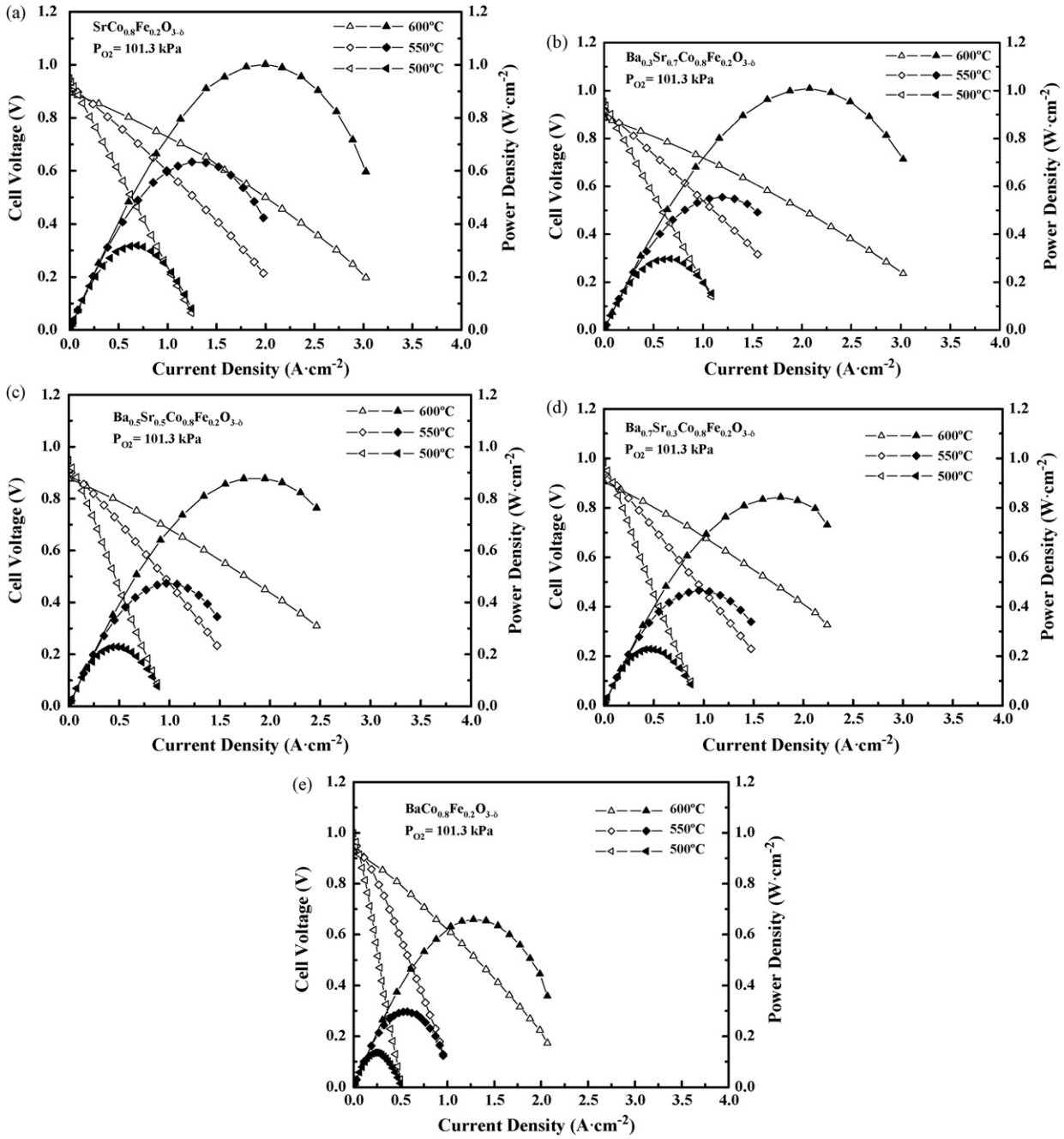

Fig. 1. The performance of the fuel cell with $Ba_{1-x}Sr_xCo_{0.8}Fe_{0.2}O_{3-\delta}$ cathodes using pure oxygen as oxidant at various temperatures (a) $SrCo_{0.8}Fe_{0.2}O_{3-\delta}$, (b) $Ba_{0.3}Sr_{0.7}Co_{0.8}Fe_{0.2}O_{3-\delta}$, (c) $Ba_{0.5}Sr_{0.5}Co_{0.8}Fe_{0.2}O_{3-\delta}$, (d) $Ba_{0.7}Sr_{0.3}Co_{0.8}Fe_{0.2}O_{3-\delta}$ and (e) $BaCo_{0.8}Fe_{0.2}O_{3-\delta}$.

provide a useful tool to improve the stability of BSCF to CO_2. In the present work, a series of BSCF with different proportion of Ba and Sr elements in A-site were synthesized and their electrochemical performance were examined both in the absence and presence of 1% CO_2 in order to examine their suitability as LT-SOFC cathode materials.

2. Experimental

The BSCF powders were prepared by a combined citrate and EDTA complexing method [25]. The electrolyte powder of $Sm_{0.1}Ce_{0.9}O_{1.95}$ (SDC) was synthesized according to the combustion method with Sm_2O_3 and CeO_2 as initial materials. The crystal structure of each BSCF composition was characterized by XRD (Rigaku/Miniflex).

The NiO–SDC (60:40 wt.%) anode-supported thin-film electrolyte fuel cells were fabricated using dry-pressing method as previously described [19]. The cathode was screen-printed on the SDC film using the slurry of BSCF, and fired at 950 °C for 2 h. The effective area of the cathode was 0.5 cm^2, and the thickness was about 20 μm.

The cell performance was evaluated by employing an in-house test station. The single cell was in situ reduced in the presence of H_2 for several hours and then the performance of the cell was measured at 500–600 °C by changing an external load. Humidified hydrogen (3% H_2O) and oxygen were supplied at a flow rate

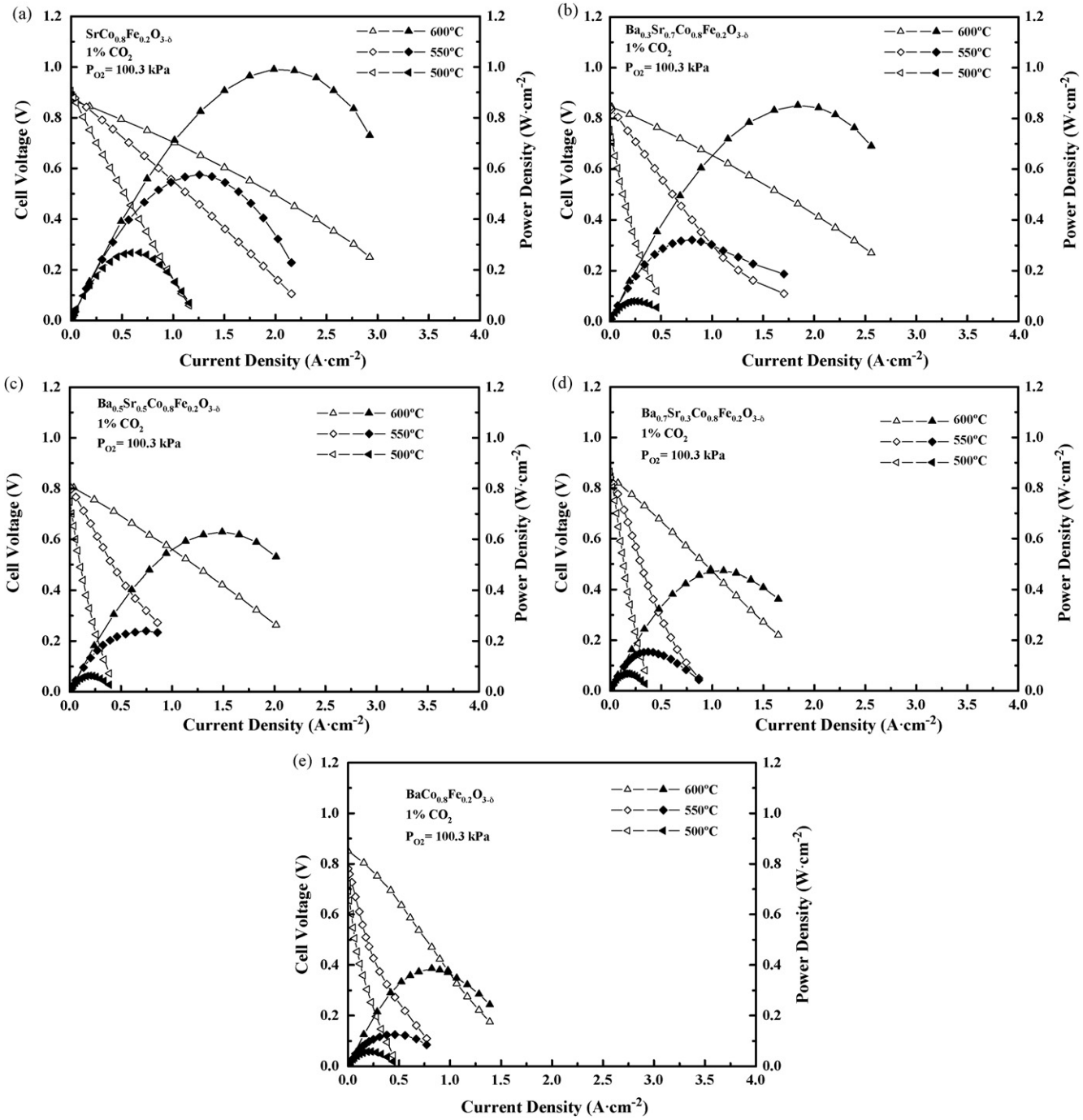

Fig. 2. The performance of the fuel cell with $Ba_{1-x}Sr_xCo_{0.8}Fe_{0.2}O_{3-\delta}$ cathode using 1% CO_2/O_2 as the oxidant at various temperatures (a) $SrCo_{0.8}Fe_{0.2}O_{3-\delta}$, (b) $Ba_{0.3}Sr_{0.7}Co_{0.8}Fe_{0.2}O_{3-\delta}$, (c) $Ba_{0.5}Sr_{0.5}Co_{0.8}Fe_{0.2}O_{3-\delta}$, (d) $Ba_{0.7}Sr_{0.3}Co_{0.8}Fe_{0.2}O_{3-\delta}$ and (e) $BaCo_{0.8}Fe_{0.2}O_{3-\delta}$.

of 100 ml min^{-1} to the anode and the cathode side, respectively. In order to investigate the influence of CO_2 on BSCF cathode, 1% CO_2 was introduced into the cathode gas line. Meanwhile, the current density at a constant voltage value of 0.7 V was recorded along with time. The electrochemical impedance spectra (EIS) measurements were carried out under open circuit conditions by using a Solartron 1287 potentiostat and a 1260 frequency response analyzer. The spectra were taken in the frequency range of 0.1 Hz to 5 kHz with signal amplitude of 10 mV.

Carbon dioxide temperature programmed desorption (TPD) was measured on the flowing reaction system using a mass spectrometer (Ominstar Balzers) as the detector, as previously described [29]. The signal of CO_2 was recorded after co-adsorption of 1% CO_2/He + 5%O_2/He gas mixture at 600 °C for 2 h.

3. Results and discussion

3.1. Cell performance both in the absence and presence of CO_2

Fig. 1 presents the *I–V* curves and the corresponding power densities of the single cell with BSCF cathodes at temperatures ranging from 500 to 600 °C under the condition of using pure

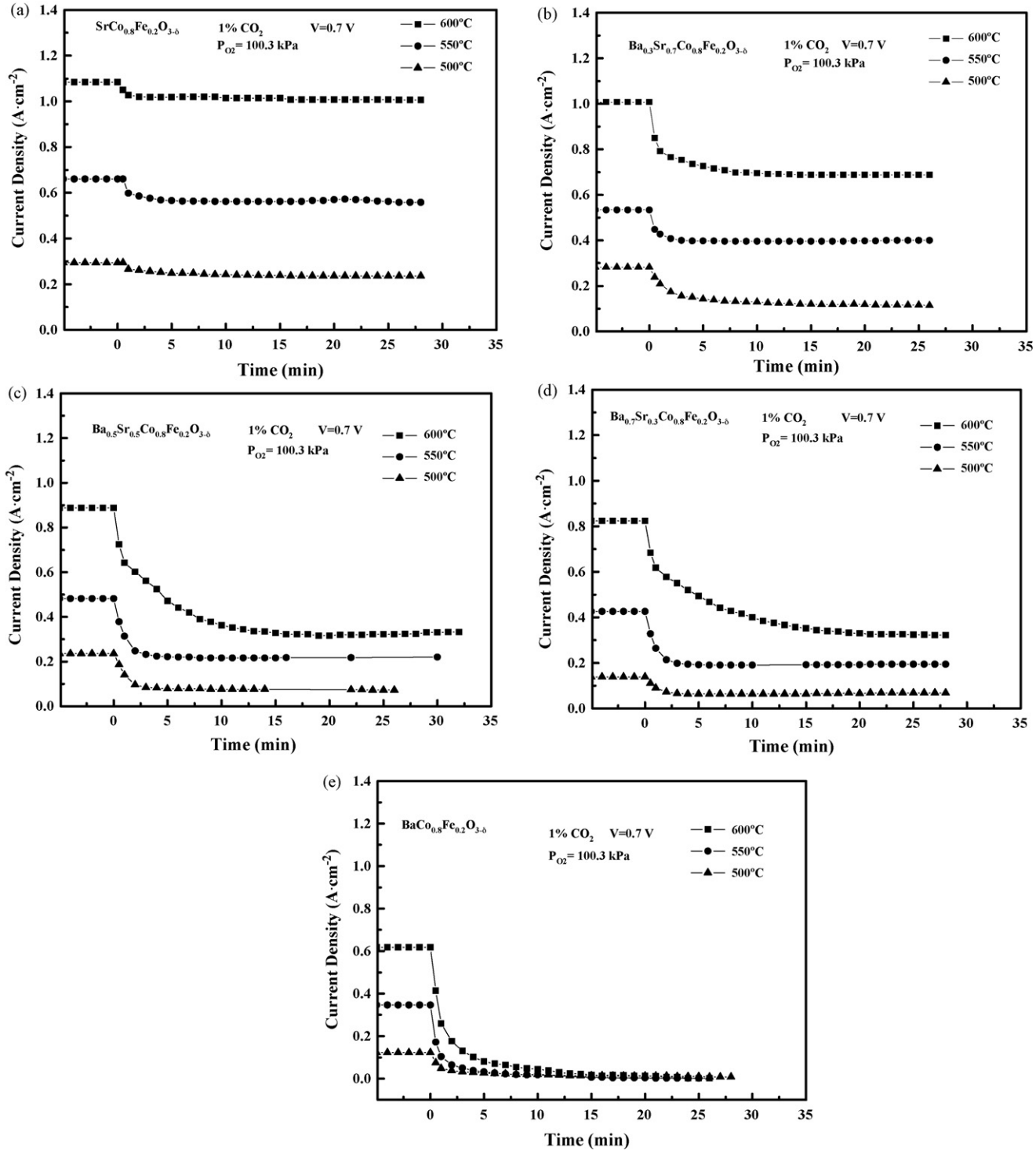

Fig. 3. Current density along with time at temperatures ranging from 500 to 600 °C with 1% of CO_2 in pure oxygen as oxidant, V = 0.7 V (a) $SrCo_{0.8}Fe_{0.2}O_{3-\delta}$, (b) $Ba_{0.3}Sr_{0.7}Co_{0.8}Fe_{0.2}O_{3-\delta}$, (c) $Ba_{0.5}Sr_{0.5}Co_{0.8}Fe_{0.2}O_{3-\delta}$, (d) $Ba_{0.7}Sr_{0.3}Co_{0.8}Fe_{0.2}O_{3-\delta}$ and (e) $BaCo_{0.8}Fe_{0.2}O_{3-\delta}$.

oxygen as the oxidant. All the cathodes exhibit high performance in the present experimental conditions. For instance, peak power densities as high as 1.01, 1.00, 0.88, 0.84 and 0.66 W cm^{-2} are obtained with $SrCo_{0.8}Fe_{0.2}O_{3-\delta}$ (SCF), $Ba_{0.3}Sr_{0.7}Co_{0.8}Fe_{0.2}O_{3-\delta}$ (BSCF3782), BSCF5582, $Ba_{0.7}Sr_{0.3}Co_{0.8}Fe_{0.2}O_{3-\delta}$ (BSCF7382) and $BaCo_{0.8}Fe_{0.2}O_{3-\delta}$ (BCF) cathodes at 600 °C, respectively. It can be seen that the SCF cathode shows the highest performance among the samples, followed by BSCF3782 and BSCF5582 cathodes. BCF cathode exhibits the lowest performance with its peak power density as 0.66, 0.30 and 0.14 W cm^{-2}, respectively at 600, 550 and 500 °C.

Fig. 2 illustrates the cell performance with different cathodes using 1% CO_2/O_2 as the oxidant. All the cells exhibit a decrease in performance as compared with that when pure oxygen was utilized as oxidant. The cell with SCF cathode remains the highest performance, and the maximum power densities (MPDs) of the cell are

0.99, 0.58 and 0.27 W cm^{-2} at 600, 550 and 500 °C, respectively. Additionally, relatively high performance is obtained for the cell with BSCF3782 and BSCF5582 cathodes since the MPD of these two cells at 600 °C are 0.85 and 0.63 W cm^{-2} comparing the values of MPD as 0.39, 0.13 and 0.06 W cm^{-2} at 600, 550 and 500 °C when the cathode of the cell is BCF. In previous investigations [19,21], we have found that even small amount of CO_2 deteriorated $Ba_{0.5}Sr_{0.5}Co_{0.8}Fe_{0.2}O_{3-\delta}$ cathode. The results presented in Fig. 2 suggest that CO_2 has a poisoning effect on $Ba_{1-x}Sr_xCo_{0.8}Fe_{0.2}O_{3-\delta}$ cathodes in the whole range of strontium doping levels. The influence of CO_2 on the samples we test, however, varies possibly due to the different compositions and structures of the samples, which will be discussed later in this paper.

3.2. Stability of current density at a constant voltage

In order to further investigate the poisoning effect of CO_2 on BSCF cathodes, O_2 was replaced by 1% CO_2/O_2 as the oxidant, and the current density at 0.7 V was recorded along with time. The results are shown in Fig. 3. It can be seen that the current density reduces rapidly due to the introduction of CO_2 in the first 2 min, and progressively decreases along with time until it reaches a steady state after a period of time. It is worth noting that the influence of CO_2 on SCF is less than that on other cathodes. For SCF, the current density at 600, 550 and 500 °C is 1.006, 0.558 and 0.236 A cm^{-2}, respectively under the condition of using 1% of CO_2/O_2 as oxidant, which corresponds to 0.078, 0.102 and 0.058 A cm^{-2} loss of the current density. The deterioration effect is aggravated with the increasing of barium content in the A-site. When the A-site is completely substituted by barium, the current density is only ~0.002 A cm^{-2} at 0.7 V at all temperatures.

3.3. XRD and SEM characterizations

Fig. 4(a) shows the XRD patterns of BSCF powders with different strontium doping levels. Strong reflection peaks with the diffractions at $2\theta = 23°$, 32°, 40°, 46°, 54° and 59° identified as typical perovskite structure [25] are presented on the XRD patterns of BSCF for $x \leq 0.5$. Weak diffraction peaks at 26.9° and 41.8°, which can be assigned to $BaCoO_{2.93}$ phase, are also observed besides the perovskite peaks for $x = 0.7$, indicating that second phase is formed in this sample. Diffractions at $2\theta = 36–40°, 41–43°, 51–55°$ and 58–60°, which can be attributed to BaO, Fe_2O_3 and some unknown phases, appear on the XRD pattern of BCF sample. It is known that the tolerance factor (t) must lie within the range of 0.8–1 in order to form a perovskite crystal structure [22]. For BCF, t is larger than 1 even when all the Fe and Co ions are of +3 state. Therefore, it is difficult to obtain BCF with pure perovskite structure. It can also be observed that the main peak around $2\theta = 32°$ of the samples shifts gradually to higher degrees when x increases from 0 to 1, suggesting that the lattice parameters decrease with increasing the strontium content, which is resulted from the substitution of small Sr^{2+} ions with large Ba^{2+} ions.

Fig. 4(b) depicts the XRD patterns of BSCF powder after being treated in 1% CO_2/O_2 at 600 °C for 30 min. By comparing with Fig. 4(a), it can be seen that no reflection peaks of newly formed chemicals occur, which is different from what was observed when BSCF was treated in CO_2/He atmosphere [29]. This is because the presence of O_2 could inhibit the reaction between CO_2 and BSCF perovskite, as has been reported previously [29].

The grain size of the starting powder was detected by SEM and the results are listed in Table 1. Generally speaking, all the samples with different compositions comprise of small particles and big agglomerates. As the barium content increases, the particles become larger. Especially for BCF, the porous agglomerates of 10–20 μm are prevail.

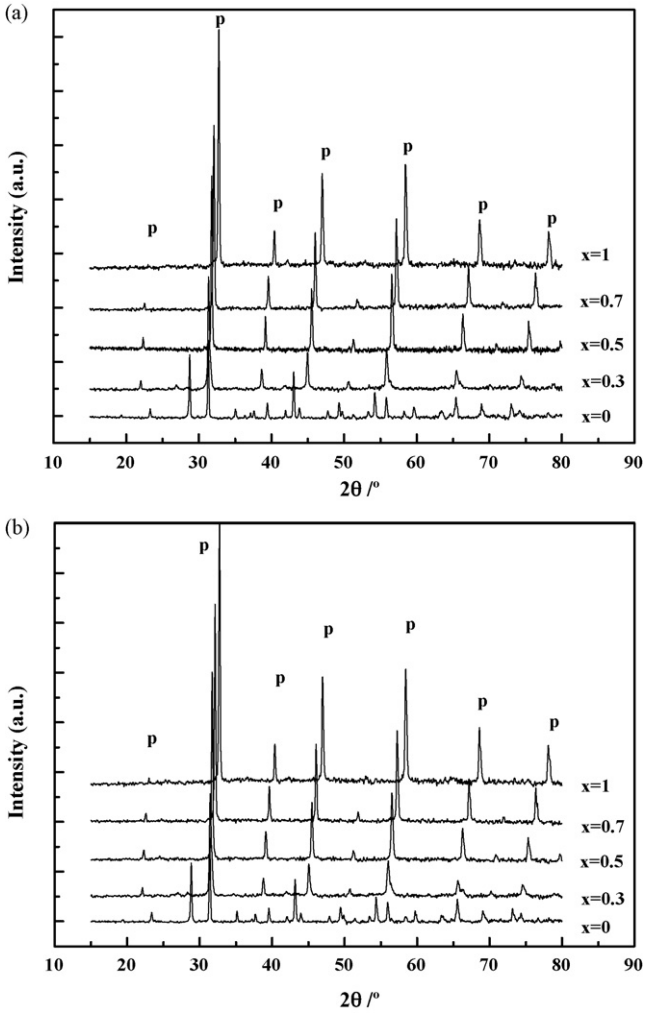

Fig. 4. (a) The XRD patterns of $Ba_{1-x}Sr_xCo_{0.8}Fe_{0.2}O_{3-\delta}$; (b) the XRD patterns of $Ba_{1-x}Sr_xCo_{0.8}Fe_{0.2}O_{3-\delta}$ after treated in 1% CO_2/O_2 for 30 min.

Fig. 5 shows the SEM micrograph of BSCF cathodes calcined at 950 °C. For the samples with $x \geq 0.3$, the cathodes show a structure with reasonable porosity and well-necked particles, having good adhesion to the electrolyte. SCF cathode contains small particles of ~2 μm and large agglomerates of ~10 μm. For the samples with $x \leq 0.7$, completely fused-together-particles are present and no boundary of the primary particles can be identified. As far as BCF is concerned, an over-sintering phenomenon and poor connection with the electrolyte are observed. Large particles over 20 μm are formed.

Fig. 6 illustrates the SEM pictures of BSCF cathodes after operated in 1% CO_2/O_2 at 600 °C. The samples show a coarsened microstructure as compared with the case of fresh ones. However, no particles related to carbonates are observed.

Table 1
Grain size of $Ba_{1-x}Sr_xCo_{0.8}Fe_{0.2}O_{3-\delta}$ powder

Sample	SCF	3782	5582	7382	BCF
Small particle (μm)	1–2	~2	2–5	~5	
Agglomerates (μm)	5–7	~7	~8	~9, ~20	10–20

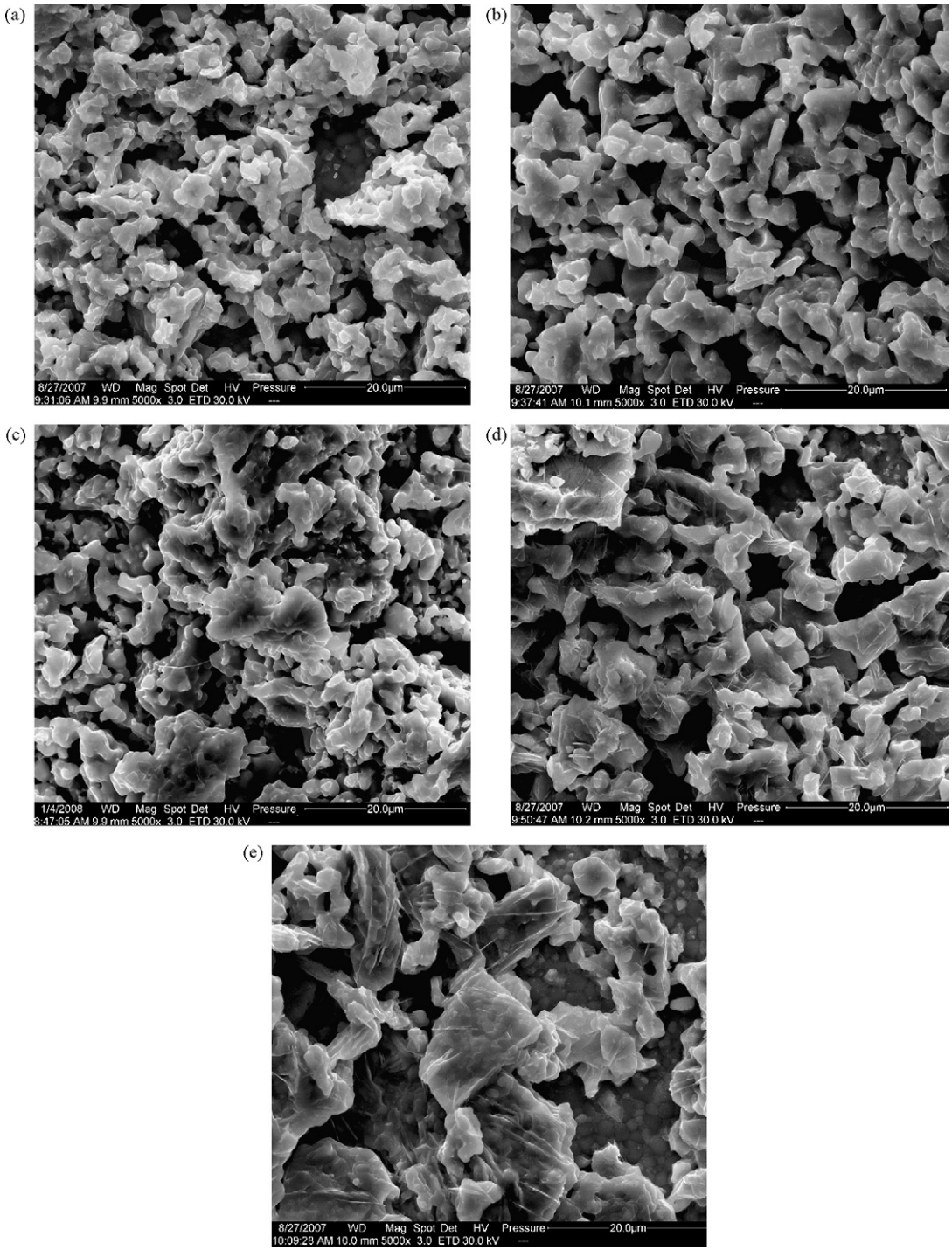

Fig. 5. SEM micrograph of the surface of $Ba_{1-x}Sr_xCo_{0.8}Fe_{0.2}O_{3-\delta}$ cathode sintered at 950 °C (a) $SrCo_{0.8}Fe_{0.2}O_{3-\delta}$, (b) $Ba_{0.3}Sr_{0.7}Co_{0.8}Fe_{0.2}O_{3-\delta}$, (c) $Ba_{0.5}Sr_{0.5}Co_{0.8}Fe_{0.2}O_{3-\delta}$, (d) $Ba_{0.7}Sr_{0.3}Co_{0.8}Fe_{0.2}O_{3-\delta}$ and (e) $BaCo_{0.8}Fe_{0.2}O_{3-\delta}$.

3.4. Impedance analysis

In Fig. 7, the impedance spectra of the fuel cell with different BSCF cathodes using O_2 or 1% CO_2/O_2 as oxidant are compared. The intercept with the real axis at high frequencies represents the ohmic resistance (R_Ω), while the intercept with the real axis at low frequencies corresponds to the total resistance of the cell (R_T). The polarization resistance (R_p) can be derived by the equation proposed by Liu and Hu [30]. The impedance of the cell at 600 °C with O_2 as oxidant is a pressed arc including two arcs. The high frequency arc can be attributed to the charge transfer process on the cathode, which is contributed by the surface contact of the cathode particles on the electrolyte surface [31–33]. On the other hand, the low-frequency arc is related to the exchange reaction of oxygen on the cathode surface [34]. The impedances of the fuel cells were measured by using a two electrode configuration. Thus, the obtained impedance was the combination of the anode, cathode and electrolyte. Since the anode and electrolyte were identical for all the cells, differences in the impedance spectra could be assigned solely to differences in the cathode at a given temperature.

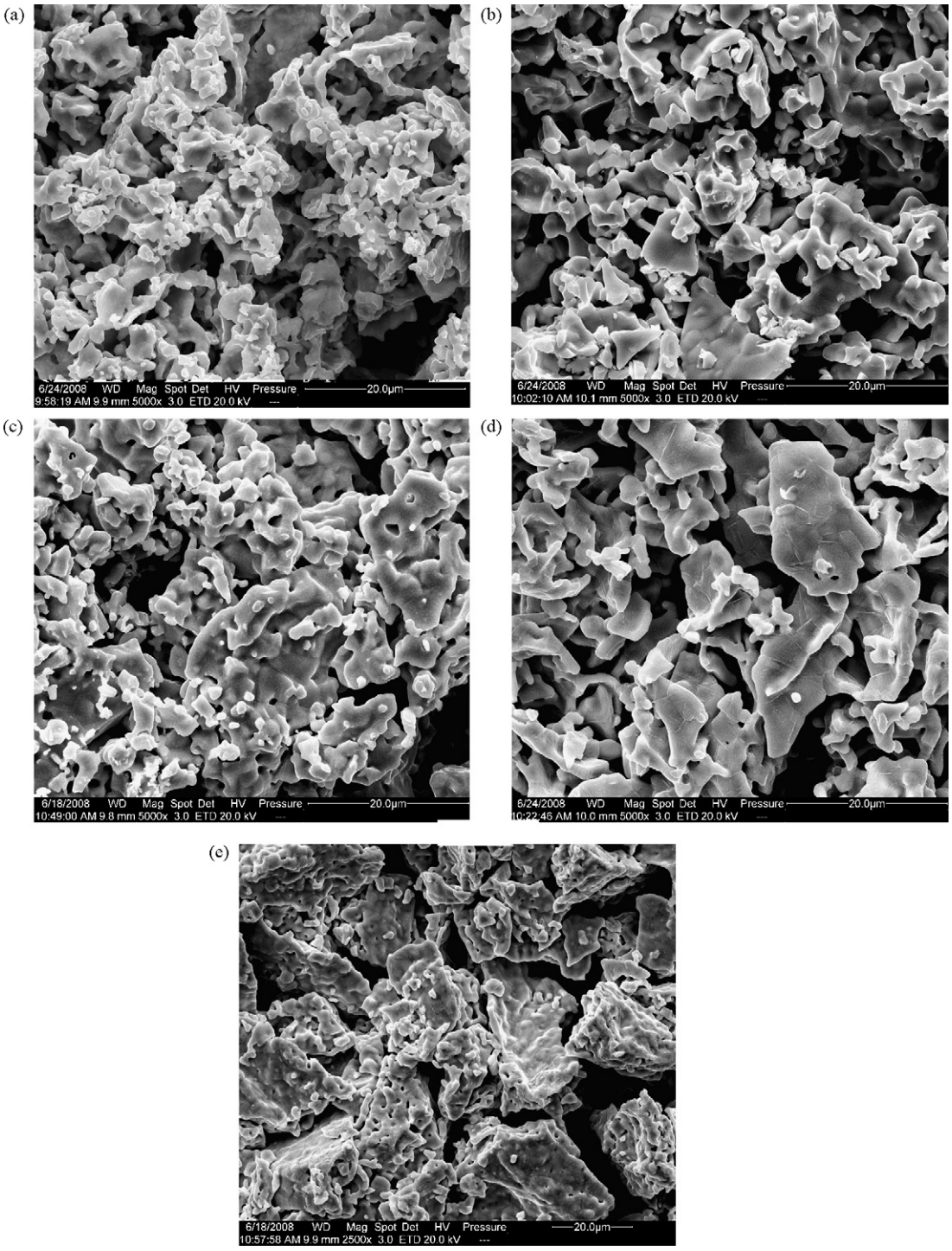

Fig. 6. SEM micrograph of the surface of $Ba_{1-x}Sr_xCo_{0.8}Fe_{0.2}O_{3-\delta}$ cathode after operated in 1% CO_2/O_2 at 600 °C for 30 min (a) $SrCo_{0.8}Fe_{0.2}O_{3-\delta}$, (b) $Ba_{0.3}Sr_{0.7}Co_{0.8}Fe_{0.2}O_{3-\delta}$, (c) $Ba_{0.5}Sr_{0.5}Co_{0.8}Fe_{0.2}O_{3-\delta}$, (d) $Ba_{0.7}Sr_{0.3}Co_{0.8}Fe_{0.2}O_{3-\delta}$ and (e) $BaCo_{0.8}Fe_{0.2}O_{3-\delta}$.

The ohmic resistance, which is from the electrolyte, electrodes and connection wires, decreases continually with the increase of strontium content. For example, the R_Ω of the cells at 600 °C is 0.171, 0.125, 0.118, 0.092 and 0.088 $\Omega\,cm^2$ when the value of x is equal to 0, 0.3, 0.5, 0.7 and 1, respectively. It was reported that BSCF with different compositions in A-site shows quite different electrical properties and its electrical conductivity elevated concomitant with the decrease of the barium doping level [27]. As reported by Wei et al. [27], the electrical conductivity of BSCF3782 and BSCF7382 at 600 °C was ~20 and ~60 $S\,cm^{-1}$, respectively. Therefore, the variance of R_Ω with different compositions could be attributed to their different electrical conductivities and different contact resistances between the cell and the silver mesh [35].

The polarization resistance increases slowly with the value of x dropping from 1 to 0.3 and then increases dramatically when the value of x equals to 0 (BCF). A similar trend was observed at all temperatures. It is known that the microstructure of the electrodes has a significant effect on the electrode properties [36–38].

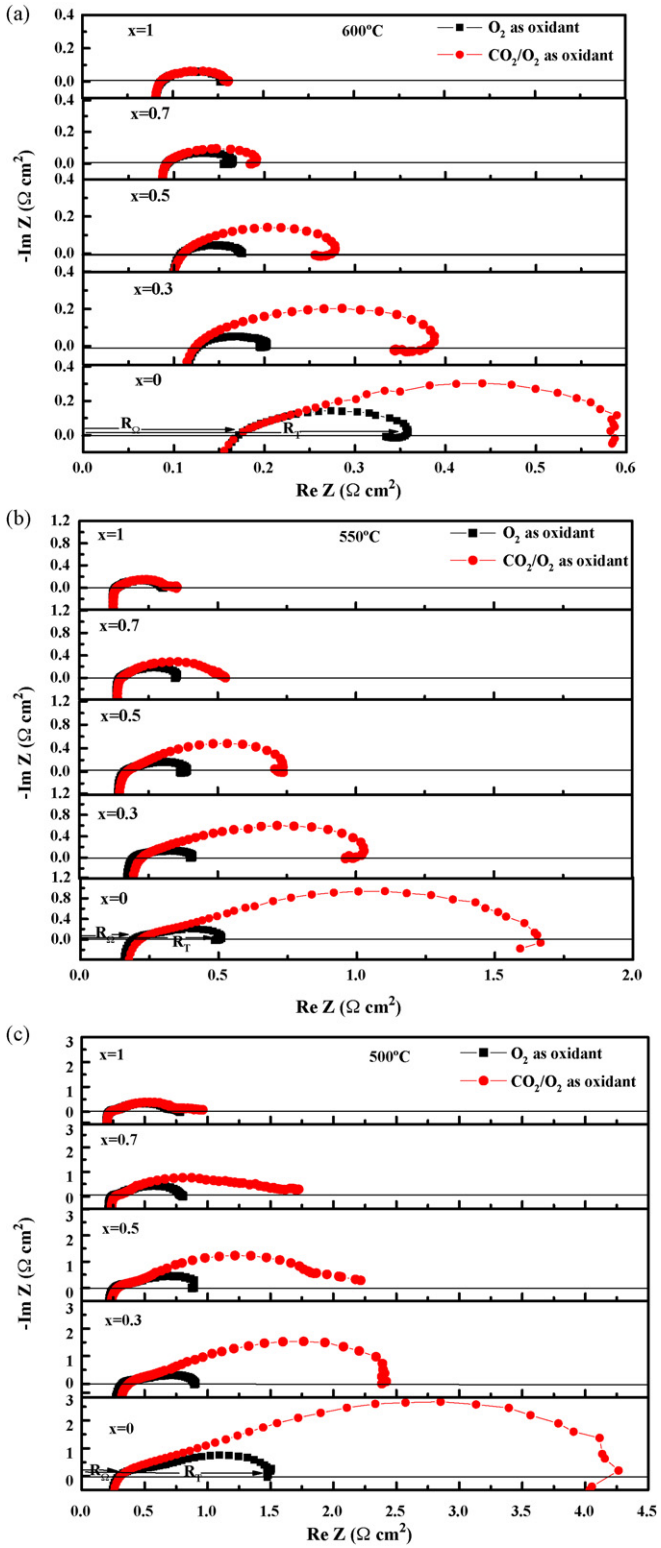

Fig. 7. Comparison of the impedance spectra of the fuel cell in the absence and presence of CO_2 at 500–600 °C. (a) 600 °C; (b) 550 °C; (c) 500 °C.

The poor microstructure led to a decrease of the electrode porosity and triple phase boundary (TPB) length, which not only prohibited the transport of oxygen but also reduced the reaction zone. As can be seen from Fig. 5, the SCF cathode shows the smallest particles which provide the highest specific surface area and

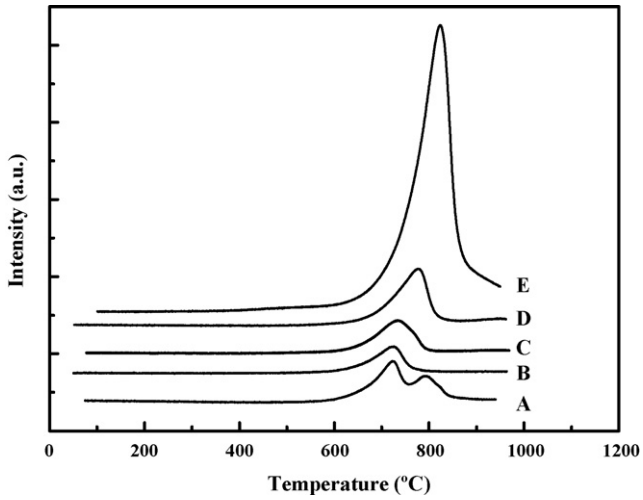

Fig. 8. CO_2-TPD profiles from $Ba_{1-x}Sr_xCo_{0.8}Fe_{0.2}O_{3-\delta}$ after CO_2–O_2 co-adsorption at 600 °C for 2 h. (A) $SrCo_{0.8}Fe_{0.2}O_{3-\delta}$; (B) $Ba_{0.3}Sr_{0.7}Co_{0.8}Fe_{0.2}O_{3-\delta}$; (C) $Ba_{0.5}Sr_{0.5}Co_{0.8}Fe_{0.2}O_{3-\delta}$; (D) $Ba_{0.7}Sr_{0.3}Co_{0.8}Fe_{0.2}O_{3-\delta}$; (E) $BaCo_{0.8}Fe_{0.2}O_{3-\delta}$.

largest TPB length. In contrast, the BCF cathode exhibits a poor microstructure with 20 μm particles. Meanwhile, the process of oxygen reduction is also affected by the electrical conductivity. Zeng et al. [39] and Wei et al. [27] reported that, the total conductivity of BSCF was improved when the strontium content increased. Moreover, the secondary phases are formed in BSCF7382 and BCF and high ohmic resistance are subsequently introduced in the system [40–42]. Therefore, the microstructure, electrical conductivity and component of the materials simultaneously affect the process of oxygen reduction.

When CO_2 was introduced into the cathode gas line, the variance of the ohmic resistance and the high-frequency arc polarization is very small. However, the low-frequency arc polarization resistance increases as compared with that under the condition of using O_2 as oxidant, especially when the strontium content is lower than 0.5. A similar phenomenon is observed at various temperatures. Combined the impedance spectra with the XRD results, it is conceivable that the existence of CO_2 mainly influences the exchange reaction of oxygen and the cathodes with higher barium contents are more susceptible to CO_2.

3.5. CO_2-TPD

According to the impedance characterization, it is reasonable to propose that the different effect of CO_2 on BSCF results from its different adsorption property on these materials. In a previous TPD investigation, it was found that the amount of CO_2 adsorbed on BSCF increased with elevated barium doping level [29]. Since the cell was operated in an oxygen-rich environment, a CO_2-TPD experiment after co-adsorption of CO_2 and O_2 was conducted in the present investigation and a similar trend is observed. As can be seen in Fig. 8, the desorption of CO_2 reaches a peak at 726.0, 733.9, 777.4 and 823.3 °C with $x = 0.7$, 0.5, 0.3 and 0. The TPD profile of SCF shows two desorption peaks at 721.7 and 789.3 °C. Meanwhile, the desorption area of CO_2 increases remarkably as the barium content increases from 0 to 1. The TPD results confirm that CO_2 is easier to be adsorbed on BSCF with higher barium content. When small Sr ions were substituted by larger Ba ions, the Fe and Co ions were prone to be oxidized from lower to higher valences to maintain the perovskite structure, which was concurrent with the creation of oxygen vacancies in order to keep the electrical neutrality [25,43], providing adsorption sites for CO_2.

It can be seen that BSCF cathode with high strontium content ($x = 1, 0.7, 0.5$) shows low ohmic and polarization resistance, high power density and high resistant to CO_2 attack. However, SCF has a high TEC and is prone to change to brownmillerite-type structure below 1073 K at P_{O_2} lower than around 0.1 atm [26]. Therefore, compositions with 50–70% strontium content are more suitable as cathode materials for LT-SOFCs.

4. Conclusions

A series of BSCF with different composition of Ba and Sr in the A-site were synthesized and their electrochemical performance were evaluated both in the absence and presence of 1% CO_2 in order to examine their suitability as LT-SOFC cathode materials. All the BSCF ($0 \leq x \leq 1$) cathodes displayed promising performance at 500–600 °C in the absence of CO_2. Increase of the strontium doping level in BSCF led to moderate decrease in the ohmic resistance and polarization resistance of the fuel cell. The presence of CO_2 had a negative effect on the performance of the fuel cell. Particularly, BSCF with higher barium content was found to be more susceptible to CO_2. Based on all these results, we propose that BSCF containing 50–70% strontium is potential cathode materials for LT-SOFCs.

Acknowledgements

The authors gratefully acknowledge financial supports from the Ministry of Science and Technology of China (Grant No. 2004CB719506, 2005CB221404 and 2006AA05z147), National Natural Science Foundation of China (Grant No.20676132) and European Committee (SOFC 600).

References

[1] O. Yamamoto, Electrochim. Acta 45 (2000) 2423–2435.
[2] S. Douvartzides, F. Coutelieris, P. Tsiakaras, J. Power Sources 114 (2003) 203–212.
[3] S. Douvartzides, F. Coutelieris, P. Tsiakaras, J. Power Sources 131 (2004) 224–230.
[4] S. Douvartzides, F. Coutelieris, A. Demin, P. Tsiakaras, Int. J. Hydrogen Energy 29 (2004) 375–379.
[5] M. Shiono, K. Kobayashi, T.L. Nguyen, K. Hosoda, T. Kato, K. Ota, M. Dokiya, Solid State Ionics 170 (2004) 1–7.
[6] B. Zhu, X.T. Yang, J. Xu, Z.G. Zhu, S.J. Ji, M.T. Sun, J.C. Sun, J. Power Sources 118 (2003) 47–53.
[7] R. Doshi, V.L. Richards, J.D. Carter, X. Wang, M. Krumpelt, J. Electrochem. Soc. 146 (1999) 1273–1278.
[8] E. Maguire, B. Gharbage, F.M.B. Marques, J.A. Labrincha, Solid State Ionics 127 (2000) 329–335.
[9] B.C.H. Steele, J. Power Sources 49 (1994) 1–14.
[10] V. Dusastre, J.A. Kilner, Solid State Ionics 126 (1999) 163–174.
[11] S. Carter, A. Selcuk, R.J. Chater, J. Kajda, J.A. Kilner, B.C.H. Steel, Solid State Ionics 53–56 (1992) 597–605.
[12] Z. Shao, S.M. Haile, Nature 431 (2004) 170–173.
[13] Z. Shao, S.M. Haile, J. Ahn, P.D. Ronney, Z. Zhan, S.A. Barnett, Nature 435 (2005) 795–798.
[14] Z. Duan, A. Yan, Y. Dong, C. You, M. Cheng, W. Yang, Chin. J. Catal. 26 (2005) 1–3.
[15] Z. Duan, M. Yang, A. Yan, Z. Hou, Y. Dong, C. You, M. Cheng, W. Yang, J. Power Sources 160 (2006) 57–64.
[16] J. Peña-Martínez, D. Marrero-López, J.C. Ruiz-Morales, B.E. Buergler, P. Nùñez, L.J. Gauckler, J. Power Sources 159 (2006) 914–921.
[17] Q.L. Liu, K.A. Khor, S.H. Chan, J. Power Sources 161 (2006) 123–128.
[18] F.S. Baumann, J. Fleig, H.-U. Habermeier, J. Maier, Solid State Ionics 177 (2006) 3187–3191.
[19] A. Yan, M. Cheng, Y. Dong, W. Yang, V. Maragou, S. Song, P. Tsiakaras, Appl. Catal. B 66 (2006) 64–71.
[20] M. Arnold, H. Wang, A. Feldhoff, J. Membr. Sci. 293 (2007) 44–52.
[21] A. Yan, V. Maragou, A. Arico, M. Cheng, P. Tsiakaras, Appl. Catal. B 76 (2007) 320–327.
[22] H. Tanaka, M. Misono, Curr. Opin. Solid State Mater. Sci. 5 (2001) 381–387.
[23] Z. Chen, R. Ran, W. Zhou, Z. Shao, S. Liu, Electrochim. Acta 52 (2007) 7343–7351.
[24] Y.H. Lim, J. Lee, J.S. Yoon, C.E. Kim, H.J. Hwang, J. Power Sources 171 (2007) 79–85.
[25] Z. Shao, G. Xiong, J. Tong, H. Dong, W. Yang, Sep. Purif. Technol. 25 (2001) 419–429.
[26] S. McIntosh, J.F. Vente, W.G. Haije, D.H.A. Blank, H.J.M. Bouwmeester, Solid State Ionics 177 (2006) 1737–1742.
[27] B. Wei, Z. Lü, X. Huang, J. Miao, X. Sha, X. Xin, W. Su, J. Eur. Ceram. Soc. 26 (2006) 2827–2832.
[28] K. Nomura, Y. Ujihira, T. Hayakawa, K. Takehira, Appl. Catal. A 137 (1996) 25–36.
[29] A. Yan, B. Liu, Y. Dong, Z. Tian, D. Wang, M. Cheng, Appl. Catal. B 80 (2008) 24–31.
[30] M. Liu, H. Hu, J. Electrochem. Soc. 143 (1996) L109–L112.
[31] F.H. van Heuveln, H.J.M. Bouwmeester, J. Electrochem. Soc. 144 (1997) 134–140.
[32] Y.J. Leng, S.H. Chan, K.A. Khor, S.P. Jiang, Int. J. Hydrogen Energy 29 (2004) 1025–1033.
[33] H.-C. Yu, F. Zhao, A.V. Virkar, K.-Z. Fung, J. Power Sources 152 (2005) 22–26.
[34] T. Kato, K. Nozaki, A. Negishi, K. Kato, A. Monma, Y. Kaga, S. Nagata, K. Takano, T. Inagaki, H. Yoshida, K. Hosoi, K. Hoshino, T. Akbay, J. Akikusa, J. Power Sources 133 (2004) 169–174.
[35] H. Lv, B. Zhao, Y. Wu, G. Sun, G. Chen, K. Hu, Mater. Res. Bull. 42 (2007) 1999–2012.
[36] Q. Li, Y. Fan, H. Zhao, L. Sun, L. Huo, J. Power Sources 167 (2007) 64–68.
[37] F. Qiang, K. Sun, N. Zhang, X. Zhu, S. Le, D. Zhou, J. Power Sources 168 (2007) 338–345.
[38] S.J. Skinner, Fuel Cells Bull. 4 (2001) 6–12.
[39] P. Zeng, Z. Chen, W. Zhou, H. Gu, Z. Shao, Z. Liu, J. Membr. Sci. 291 (2007) 148–156.
[40] V.V. Kharton, A.A. Yaremchenko, E.N. Naumovich, J. Solid State Electrochem. 3 (1999) 303–326.
[41] M. Liu, Z. Wu, Solid State Ionics 107 (1998) 105–110.
[42] T. Kenjo, Y. Kanehira, Solid State Ionics 148 (2002) 1–14.
[43] L.-W. Tai, M.M. Nasrallah, H.U. Anderson, D.M. Sparlin, S.R. Schlin, Solid State Ionics 76 (1995) 259–271.